Preprints.org

Article

Not peer-reviewed version

Automated Design of Multi-Layer Planar Transformers: An EDA Tool Based on a Constraint-Preserving Genetic Algorithm

Dejun Ba , Yihe Wang , Faxin Yu , Xiaofeng Lyu *

Posted Date: 13 May 2026

doi: 10.20944/preprints202605.0891.v1

Keywords: Multi-Layer Planar Transformers; high-frequency magnetic components; magnetomotive force; genetic algorithm; thermal hotspots; leakage inductance

Preprints.org is a free multidisciplinary platform providing preprint service that is dedicated to making early versions of research outputs permanently available and citable. Preprints posted at Preprints.org appear in Web of Science, Crossref, Google Scholar, Scilit, Europe PMC, OpenAlex.

Copyright: This open access article is published under a Creative Commons CC BY 4.0 license, which permit the free download, distribution, and reuse, provided that the author and preprint are cited in any reuse.

Preprints.org (www.preprints.org) | NOT PEER-REVIEWED | Posted: 13 May 2026 doi:10.20944/preprints202605.0891.v1

Disclaimer/Publisher's Note: The statements, opinions, and data contained in all publications are solely those of the individual author(s) and contributor(s) and not of MDPI and/or the editor(s). MDPI and/or the editor(s) disclaim responsibility for any injury to people or property resulting from any ideas, methods, instructions, or products referred to in the content.

Article

Automated Design of Multi-Layer Planar Transformers: An EDA Tool Based on a Constraint-Preserving Genetic Algorithm

Dejun Ba, Yihe Wang, Faxin Yu and Xiaofeng Lyu *

School of Aeronautics and Astronautics, Zhejiang University, Hangzhou 310058, China

* Correspondence: xiaofeng.lyu@zju.edu.cn

Abstract

Inhomogeneous magnetic field distributions in high-frequency planar transformers frequently cause severe localized thermal hotspots and elevated leakage inductance. Traditional interleaved winding designs rely heavily on empirical trial-and-error, which becomes computationally prohibitive for multi-layer parallel structures due to the factorial "curse of dimensionality." To address this bottleneck, this paper proposes a universal, data-driven optimization methodology. First, a quantitative one-dimensional prefix-sum model is established to correlate winding arrangements with spatial magnetomotive force (MMF) distributions, effectively simplifying the electromagnetic evaluation. Subsequently, a customized Genetic Algorithm (GA) framework, featuring physical-constraint-preserving operators such as Order Crossover (OX), is introduced to efficiently navigate the high-dimensional discrete search space. Using an extreme 26-layer complex parallel winding configuration (Np:Ns = 9:2) as a primary case study, the proposed GA method effectively bypasses over 1.5 million permutations, converging to the global optimum within 100 generations. The optimized structure achieves profound peak-shaving, drastically reducing both the peak MMF and total uncoupled magnetic energy area. This methodology provides a systematic, computationally lightweight EDA solution that fundamentally replaces empirical trial-and-error in the design of high-frequency magnetic components.

Keywords: Multi-Layer Planar Transformers; high-frequency magnetic components; magnetomotive force; genetic algorithm; thermal hotspots; leakage inductance

1. Introduction

Driven by the rapid proliferation of renewable energy systems, electric vehicle (EV) fast-charging infrastructures, and hyperscale AI data centers, modern power conversion systems are aggressively pursuing ultra-high power density and extreme energy efficiency [1–3]. High-frequency planar transformers (HFPTs) have emerged as indispensable components in this paradigm shift, attributed to their low-profile geometries, superior thermal management capabilities, and exceptional parasitic parameter consistency enabled by automated manufacturing [4,5]. However, the integration of wide-bandgap (WBG) power devices facilitates switching frequencies reaching the megahertz (MHz) range [6,7], which pushes the electromagnetic performance of conventional planar magnetic components to their physical limits [8].

At MHz-level frequencies, electromagnetic phenomena that were once negligible start to dominate the loss mechanism. Non-uniform distributions of magnetic field intensity (H) and flux density (B) trigger localized magnetic saturation and significantly enlarged hysteresis loops within core materials [9,10]. Concurrently, the thin conductive layers in PCB-based windings exacerbate the skin and proximity effects, causing high-frequency currents to crowd at the surfaces and edges [11,12]. This uneven current density not only amplifies AC copper losses but also leads to severe localized thermal hotspots [13]. Furthermore, uncoupled leakage flux concentrates at the winding

© 2026 by the author(s). Distributed under a Creative Commons CC BY license.

Preprints.org (www.preprints.org) | NOT PEER-REVIEWED | Posted: 13 May 2026 doi:10.20944/preprints202605.0891.v1

boundaries or air gaps, elevating leakage inductance and degrading the overall system reliability. A typical planar transformer utilizes a low-profile magnetic core (e.g., EE-core) to enclose multiple printed circuit board (PCB) winding layers. As illustrated in Figure 1a, conventional planar designs often employ a segregated stacking configuration, which severely exacerbates the proximity effect and current crowding. To mitigate these high-frequency copper losses and suppress leakage inductance, interleaved winding configurations [see Figure 1b] are commonly adopted [14–16]. Nevertheless, current industrial design practices remain heavily reliant on empirical trial-and-error and labor-intensive finite element analysis (FEA) iterations, which lack systematic and quantitative optimization metrics. This inefficiency is critically amplified in high-current applications where multiple thin copper layers must be paralleled to construct a single electrical turn to suppress skin effects. As the number of physical layers (N) increases, the structural complexity bypasses the reach of manual intuition, creating a massive design space that cannot be navigated efficiently using traditional methods [17]. The fundamental mathematical obstacle in optimizing such structures is the "curse of dimensionality." As the layer count scales, the number of possible permutations for primary and secondary layers expands factorially, resulting in an $\mathcal{O}(N!)$ computational complexity. Evaluating the full permutation matrix via exhaustive search is computationally prohibitive and memory-intensive, especially for high-turn-count or multi-parallel designs [18]. Consequently, there is an urgent need for a universal, scalable optimization framework that can bypass this factorial bottleneck and provide a data-driven path to identify the global absolute optimum.

To bridge this critical gap, this paper proposes a heuristic optimization methodology based on a customized Genetic Algorithm (GA) [19]. The core innovation lies in transforming the complex electromagnetic evaluation into a computationally lightweight one-dimensional (1D) prefix-sum operation, which directly correlates spatial layer sequences with magnetomotive force (MMF) distribution. By targeting the minimization of Peak MMF (m) and Total MMF Area (n), the GA navigates high-dimensional discrete spaces with exceptional efficiency. The proposed methodology entirely replaces empirical trial-and-error, offering power electronics engineers an automated EDA tool to maximize the performance of high-frequency magnetic components [20].

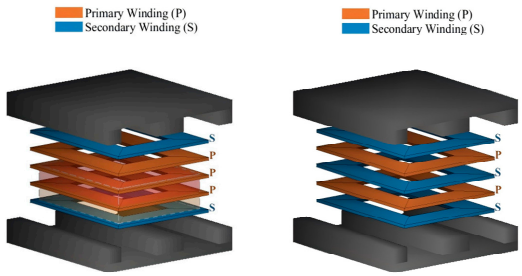

Figure 1. 3D exploded views of the multi-layer planar transformer with an EE-core: (a) conventional segregated winding stack, and (b) optimized interleaved winding stack..

2. Theoretical Modeling of Winding and Spatial Magnetic Field Distribution

In the design of high-frequency planar transformers, minute variations in the physical winding arrangement lead to severe reconstructions of the internal electromagnetic field distribution, which subsequently dictates the AC resistance (R_{AC}) and leakage inductance (L_k). Starting from fundamental electromagnetic laws, this section establishes a one-dimensional (1D) spatial analytical model for high-frequency planar transformers, derives the quantitative relationship between the inter-layer magnetic field and physical losses, and ultimately abstracts this into discrete sequence optimization objectives.

© 2026 by the author(s). Distributed under a Creative Commons CC BY license.

Preprints.org (www.preprints.org) | NOT PEER-REVIEWED | Posted: 13 May 2026 doi:10.20944/preprints202605.0891.v1

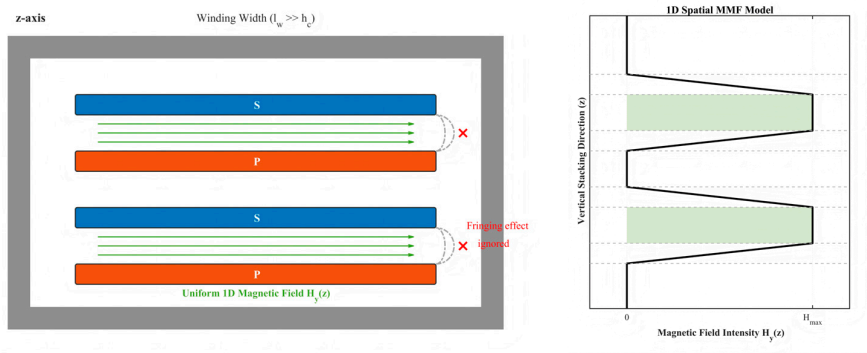

(**a**) (**b**)

Figure 2. The 1D magnetic field distribution for planar transformers: (a) physical approximation neglecting fringing effects where $l_w \gg h_c$, and (b) the mapped spatial MMF profile $H_y(z)$ used for quantitative loss evaluation.

2.1. 1D Magnetic Field Boundary Constraints

In the megahertz (MHz) frequency range, since the winding width (l_w) of a planar transformer is typically much larger than the copper foil thickness and inter-layer gap distance, the fringing effect can be neglected. Consequently, the electromagnetic field within the winding window can be approximated as a 1D distribution model along the vertical stacking direction (z-axis).According to Ampere's Circuital Law from Maxwell's equations, under the quasi-static electromagnetic field approximation (ignoring the displacement current), the line integral of the magnetic field intensity $\boldsymbol{H}$ around a closed loop equals the total conduction current enclosed:

$$\oint_l \boldsymbol{H} \cdot d\boldsymbol{l} = \iint_S \boldsymbol{J} \cdot d\boldsymbol{S} = \sum I_{enclosed} \tag{1}$$

In a transformer comprising N physical winding layers, let the bottom insulation boundary be $z = 0$. Due to the high permeability of the magnetic core ($\mu_r \gg 1$), the magnetic field intensity at the upper and lower boundaries of the winding window is considered to be zero. Therefore, the boundary condition establishing the global Ampere-turn balance is given by:

$$\sum_{i=1}^{N} N_i I_i = 0 \tag{2}$$

Let the equivalent number of turns of the i-th physical winding layer be N_i, and the current flowing through it be I_i (primary currents are defined as positive, secondary currents as negative). In the 1D model, the magnetic field intensity vector $\boldsymbol{H}$ solely possesses a horizontal component (y-axis), denoted as $H_y(z)$.

For the dielectric insulation gap located between the k-th and $(k+1)$-th winding layers (denoted by coordinate z_k), constructing a rectangular integration loop along the winding width l_w yields the localized spatial Magnetomotive Force (MMF) F_k within that gap:

$$F_k = \int_0^{z_k} J(z)dz = \sum_{i=1}^{k} N_i I_i \tag{3}$$

Consequently, the uniform magnetic field intensity H_k within the k-th gap can be analytically expressed as the discrete prefix-sum of all preceding current excitations:

© 2026 by the author(s). Distributed under a Creative Commons CC BY license.

Preprints.org (www.preprints.org) | NOT PEER-REVIEWED | Posted: 13 May 2026 doi:10.20944/preprints202605.0891.v1

$$H_k = \frac{F_k}{l_w} = \frac{1}{l_w}\sum_{i=1}^{k} N_i I_i \quad (1 \le k \le N) \tag{4}$$

This formula rigorously demonstrates from a mathematical standpoint that the magnetic field intensity in any specific inter-layer gap is strictly determined by the permutation sequence of the winding layers.

2.2. Mathematical Characterization of Physical Loss Mechanisms

The distortion of the magnetic field distribution H_k severely degrades the high-frequency performance of the transformer from both energy storage and thermal stress perspectives.

1. Energy Integral Derivation of Leakage InductanceLeakage inductance essentially characterizes the leakage magnetic energy that does not participate in the primary-to-secondary energy transfer. According to electromagnetic energy theory, the total magnetic field energy W_m stored within the winding window is:

$$W_m = \frac{1}{2} L_k I_{pri}^2 = \frac{1}{2}\iiint_V \mu_0 \,|\, \boldsymbol{H} \,|^2 \, dV \tag{5}$$

where μ_0 is the vacuum permeability and I_{pri} is the primary reference current. By discretizing the integration domain into individual insulation gaps (assuming gap thickness d_{gap} and average turn length l_T), the leakage inductance can be quantitatively expressed as:

$$L_k \approx \frac{\mu_0 l_T d_{gap}}{l_w I_{pri}^2}\sum_{k=1}^{N} H_k^2 \tag{6}$$

This derivation indicates that leakage inductance is strictly proportional to the spatial accumulation of the squared magnetic field intensity across all inter-layer gaps.

2.3. Loss Derivation of High-Frequency Proximity Effect

Under high-frequency excitation, the alternating magnetic field H_k induces intense eddy currents within the adjacent thin copper foils. According to the 1D Dowell's theory, the proximity effect loss density $P_{pe,k}$ in a single copper layer caused by the external magnetic field is:

$$P_{pe,k} \propto \frac{\omega^2 \mu_0^2 h_c^3 l_T}{24\rho} H_k^2 \tag{7}$$

where ω is the angular frequency, h_c is the copper foil thickness, and ρ is the resistivity. For the central winding layer located at the maximum magnetic field intensity H_{max}, the localized extreme loss it endures is:

$$P_{local\_max} \propto \max_{1\le k\le N}(H_k^2) \tag{8}$$

This formula reveals that the localized hotspot temperature is directly governed by the square of the spatial magnetic field peak.

2.4. Discrete Dimensionality Reduction and Heuristic Optimization Objectives

Based on the derivations of the aforementioned physical energy equations, the complex electromagnetic field optimization problem can be fully decoupled into the mathematical optimization of the discrete sequence H_k. To eliminate the interference of specific current values, normalized excitation coefficients are introduced.

© 2026 by the author(s). Distributed under a Creative Commons CC BY license.

Preprints.org (www.preprints.org) | NOT PEER-REVIEWED | Posted: 13 May 2026 doi:10.20944/preprints202605.0891.v1

For a transformer with e parallel primary layers, f parallel secondary layers, and a turns ratio of $n_p : n_s$, the array element c_i for a normalized physical layer is defined as:

$$c_i = \begin{cases} \frac{n_s}{e}, & \text{if the } i\text{-th layer is Primary (P)} \\ -\frac{n_p}{f}, & \text{if the } i\text{-th layer is Secondary (S)} \end{cases} \tag{9}$$

This definition naturally satisfies the Ampere-turn balance constraint:

$$e \cdot (\frac{n_s}{e}) + f \cdot (-\frac{n_p}{f}) = 0 \tag{10}$$

A dimensionless 1D prefix-sum array $Y = [y_1, y_2, \ldots, y_N]$ is constructed, with its recursive formula being:

$$y_k = \sum_{i=1}^{k} c_i \quad (y_0 = 0, y_N = 0) \tag{11}$$

Mapping back to the physical derivations in Section 2.3, two core mathematical optimization indicators are established here to guide heuristic algorithms (e.g., Genetic Algorithm):

Objective 1: Suppressing Localized Hotspots (Based on the Maximum Magnetic Field Equation)Extract the Peak MMF indicator m to depress the spatial MMF envelope:

$$m = \max_{1 \le k \le N} | y_k | \tag{12}$$

Objective 2: Minimizing Leakage Inductance and Global Copper Loss (Based on the Energy Integral Equation)Extract the Total MMF Area indicator n to limit the global accumulation of reactive magnetic energy:

$$n = \sum_{k=1}^{N} | y_k | \tag{13}$$

At this juncture, the multi-physics coupled high-frequency transformer design problem is theoretically and rigorously reduced to a dual-objective mathematical extremum problem concerning the discrete multiset sequence C: min(m, n).

3. Heuristic Optimization Algorithm for Winding Sequences

Building upon the discrete one-dimensional magnetic field model established in the previous section, the multi-physics synergistic design of high-frequency planar transformers has been rigorously abstracted into a mathematical extremum problem seeking the optimal winding sequence. However, facing the massive search space induced by multi-layer parallel structures, conventional exhaustive methods and empirical designs encounter an insurmountable computational bottleneck.

This chapter proposes a heuristic optimization framework based on a customized Genetic Algorithm (GA) to efficiently and stably search for the global optimum in a high-dimensional discrete space.

3.1. Asymptotic Complexity Derivation of the Discrete State Space

As established, the winding arrangement is a permutation problem of a multiset S containing N_{Lp} primary layers and N_{Ls} secondary layers, with the total layer count $N = N_{Lp} + N_{Ls}$. The total capacity of this discrete search space Ω is:

© 2026 by the author(s). Distributed under a Creative Commons CC BY license.

Preprints.org (www.preprints.org) | NOT PEER-REVIEWED | Posted: 13 May 2026 doi:10.20944/preprints202605.0891.v1

$$\Omega_{total} = \binom{N_{Lp} + N_{Ls}}{N_{Lp}} = \frac{N!}{N_{Lp}!N_{Ls}!} \tag{14}$$

To rigorously reveal the mathematical essence of the "Curse of Dimensionality," Stirling's Approximation $n! \approx \sqrt{2\pi n}(\frac{n}{e})^n$ is introduced for asymptotic complexity analysis. Assuming the layer counts maintain a constant ratio, let $N_{Lp} = \alpha N$ and $N_{Ls} = (1-\alpha)N$, where $\alpha \in (0,1)$. Applying Stirling's approximation and evaluating the logarithmic limit yields the growth rate of the state space:

$$\lim_{N\to\infty} \frac{1}{N} \ln \Omega_{total} = -\alpha \ln \alpha - (1-\alpha)\ln(1-\alpha) \tag{15}$$

The right side of the equation corresponds to the information entropy function $\mathcal{H}(\alpha)$ of a binomial distribution. When $\alpha = 0.5$ (representing extreme interleaving where primary and secondary layers are nearly equal), the entropy reaches its maximum value of $\ln 2$. Consequently, the asymptotic complexity of the search space strictly follows an exponential explosion of $\mathcal{O}(2^N)$. This derivation proves from a mathematical limit perspective that as parallel layers scale, deterministic exhaustive search inevitably confronts a singularity of computational time and memory overflow, validating the heuristic architecture as the sole viable solution path.

3.2. Mapping of the Fitness Function and Constraint Space

In heuristic search, the fitness function $Fitness(C)$ serves as the exclusive gradient guiding the population toward the target. Based on the prefix-sum array $Y = [y_1, \ldots, y_N]$, a smoothed reciprocal fitness function is constructed:

$$Fitness(C) = \frac{1}{w_1 \cdot \max_{1\le k\le N} |y_k| + w_2 \cdot \sum_{k=1}^{N} |y_k| + \epsilon} \tag{16}$$

where $w_1 \gg w_2$ to guarantee the absolute priority of localized hotspot suppression (peak-shaving), and $\epsilon \to 0^+$ prevents zero-division singularities. Simultaneously, the algorithm must strictly operate within the physical manifold space Ω_{valid} defined by the Ampere-turn balance constraint. Any valid chromosome $C = [c_1, \ldots, c_N]$ must satisfy the identity equation:

$$\sum_{i=1}^{N} c_i = 0 \quad \forall C \in \Omega_{valid} \tag{17}$$

To conduct efficient neighborhood searches within Ω_{valid}, the Swap Mutation operator is employed. Suppose that during an iteration, the a-th and b-th loci ($a < b$) of chromosome C are selected for gene value exchange.

According to the prefix-sum model $y_k = \sum_{i=1}^{k} c_i$, swapping c_a and c_b induces the following piecewise perturbation in the new prefix-sum array y'_k:

$$y'_k = \begin{cases} y_k, & 1 \le k < a \\ y_k - c_a + c_b, & a \le k < b \\ y_k, & b \le k \le N \end{cases} \tag{18}$$

© 2026 by the author(s). Distributed under a Creative Commons CC BY license.

Preprints.org (www.preprints.org) | NOT PEER-REVIEWED | Posted: 13 May 2026 doi:10.20944/preprints202605.0891.v1

This mathematical derivation uncovers a critical algorithmic advantage: A single swap mutation exclusively imposes a local algebraic translation ($\Delta y = c_b - c_a$) on the MMF within the interval $[a, b-1]$, while exerting strictly zero influence on the magnetic field distribution outside this range.

Consequently, when evaluating the fitness of mutated individuals, the time complexity plummets from $\mathcal{O}(N)$ (for reconstructing the entire array) to a locally updated $\mathcal{O}(b-a)$. This computational dimensionality reduction based on local perturbation significantly accelerates the GA's evaluation speed across massive spaces.

3.3. Global Convergence Proof Based on Markov Chain Theory

To theoretically guarantee that the proposed GA can escape local optima and ultimately lock onto the globally optimal interleaved sequence, a Markov Chain convergence model incorporating the Elitism Strategy is introduced.

Let each generational population $Pop(t)$ be considered a Markov state within the state space, governed by a transition probability matrix $\boldsymbol{P}$. The set of globally optimal solutions is defined as $\Omega_{opt} = \{C \in \Omega_{valid} \mid Fitness(C) = F_{max}\}$.

In canonical GA without elitism, due to the stochastic nature of crossover and mutation, the transition matrix $\boldsymbol{P}$ is strictly positive; the system is ergodic but does not guarantee convergence. Upon integrating the elitism strategy, the individual with the highest fitness in generation t is unconditionally preserved into generation $t+1$. Mathematically, this enforces a monotonically non-decreasing constraint:

$$P(\max Fitness(Pop(t+1)) \geq \max Fitness(Pop(t))) = 1 \tag{19}$$

According to Rudolph's convergence theorem, the aforementioned transition matrix constitutes an Absorbing Markov Chain. As the number of iterations $t \to \infty$, the probability limit of the evolutionary sequence falling into the optimal absorbing barrier converges to 1:

$$\lim_{t \to \infty} P(Pop(t) \cap \Omega_{opt} \neq \varnothing) = 1 \tag{20}$$

This Markov Chain proof provides unshakeable mathematical completeness, confirming the absolute validity of the proposed algorithm in optimizing the complex parallel structures of high-frequency transformers.

4. Case Study Validation and System-Level Evaluation

4.1. Validation Setup and Evaluation Methodology

To rigorously validate the effectiveness of the proposed Genetic Algorithm (GA)-based winding optimization methodology, this chapter maps the theoretically derived mathematical sequences into physical transformer models and conducts multi-dimensional cross-validation. In the simulation domain, Ansys Maxwell 2D FEA software is utilized to extract high-fidelity spatial magnetic field distributions, current densities within the winding window, corroborating the 1D prefix-sum mathematical model proposed in Section 2. In the experimental domain, multiple planar transformer prototypes with different winding sequences were fabricated and integrated into a megahertz-level DC-DC power converter platform for system-level performance evaluation.

4.2. Case 1: Baseline Verification for Non-Parallel and Low-Parallel Windings

To intuitively demonstrate the mapping between the spatial Magnetomotive Force (MMF) distribution and the physical winding arrangement, baseline configurations with turns ratios of Np:Ns = 3:2 are first selected for comparative analysis.

© 2026 by the author(s). Distributed under a Creative Commons CC BY license.

Preprints.org (www.preprints.org) | NOT PEER-REVIEWED | Posted: 13 May 2026 doi:10.20944/preprints202605.0891.v1

For Np:Ns = 3:2 configuration, three models are constructed: the conventional segregated stack (Worst-case baseline), the manually interleaved stack (Suboptimal baseline), and the GA-optimized stack (Best-case) are compared in Figure 3.

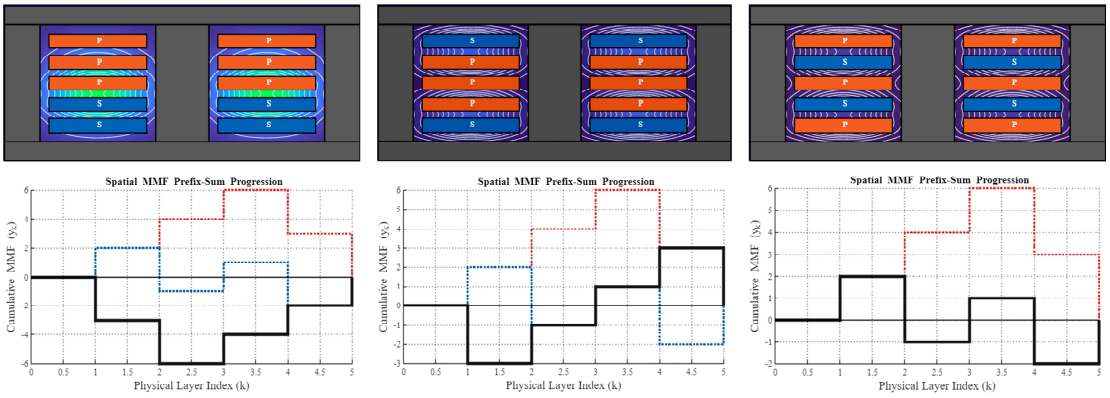

(**a**) (**b**) (**c**)

Figure 3. Comparison of winding configurations and MMF prefix-sum progressions (Np:Ns = 3:2): (**a**) segregated baseline; (**b**) manually interleaved baseline; (**c**) GA-optimized structure .

In Figure 3, the spatial MMF prefix-sum progression curves extracted via FEA reveal that the conventional segregated arrangement leads to a severe monotonic accumulation of Ampere-turns, culminating in a massive MMF peak (m) at the geometric center of the window. This extreme field concentration exponentially amplifies the high-frequency proximity effect ($P_{eddy} \propto m^2$), generating catastrophic localized hotspots. While the manually interleaved structure partially disrupts this monotonic buildup, its macroscopic asymmetry still leaves substantial localized magnetic peaks.In contrast, the global optimum generated by the proposed GA establishes perfect macroscopic symmetry. The high-frequency alternating currents of the primary and secondary windings achieve localized "neutralization," strictly clamping the MMF progression curve within the theoretical minimum envelope.

To strictly validate the theoretical derivations of the MMF prefix-sum model, 2D Finite Element Analysis (FEA) was conducted using Ansys Maxwell. The simulation was performed at a high frequency of 2 MHz, with a primary excitation current of 2 A and a secondary current of 3 A. The electromagnetic field contours of the conventional segregated structure (worst-case) and the GA-optimized interleaved structure (best-case) are compared in Figure 4.

In the segregated baseline [Figure 4a,c,e], the monotonic accumulation of Ampere-turns creates a massive magnetic peak at the window center ($H_{max} = 1302.3$ A/m, $B_{max} = 1636.5\ \mu$T). This intense field induces severe high-frequency proximity effects, squeezing the current to the inner surfaces with a peak density of $J_{max} = 3.52 \times 10^7$ A/m^2, which inevitably causes localized thermal runaway. Conversely, the GA-optimized structure [Figure 4b,d,f] achieves perfect macroscopic symmetry, effectively neutralizing local Ampere-turns. The peak magnetic field is drastically suppressed to 574.4 A/m (a 55.9% reduction), uniformly distributing the magnetic energy. Consequently, the severe current crowding is eliminated, plunging the peak current density to 1.34×10^7 A/m^2. These results physically verify the algorithm's superiority in minimizing leakage energy and high-frequency copper losses.

© 2026 by the author(s). Distributed under a Creative Commons CC BY license.

Preprints.org (www.preprints.org) | NOT PEER-REVIEWED | Posted: 13 May 2026 doi:10.20944/preprints202605.0891.v1

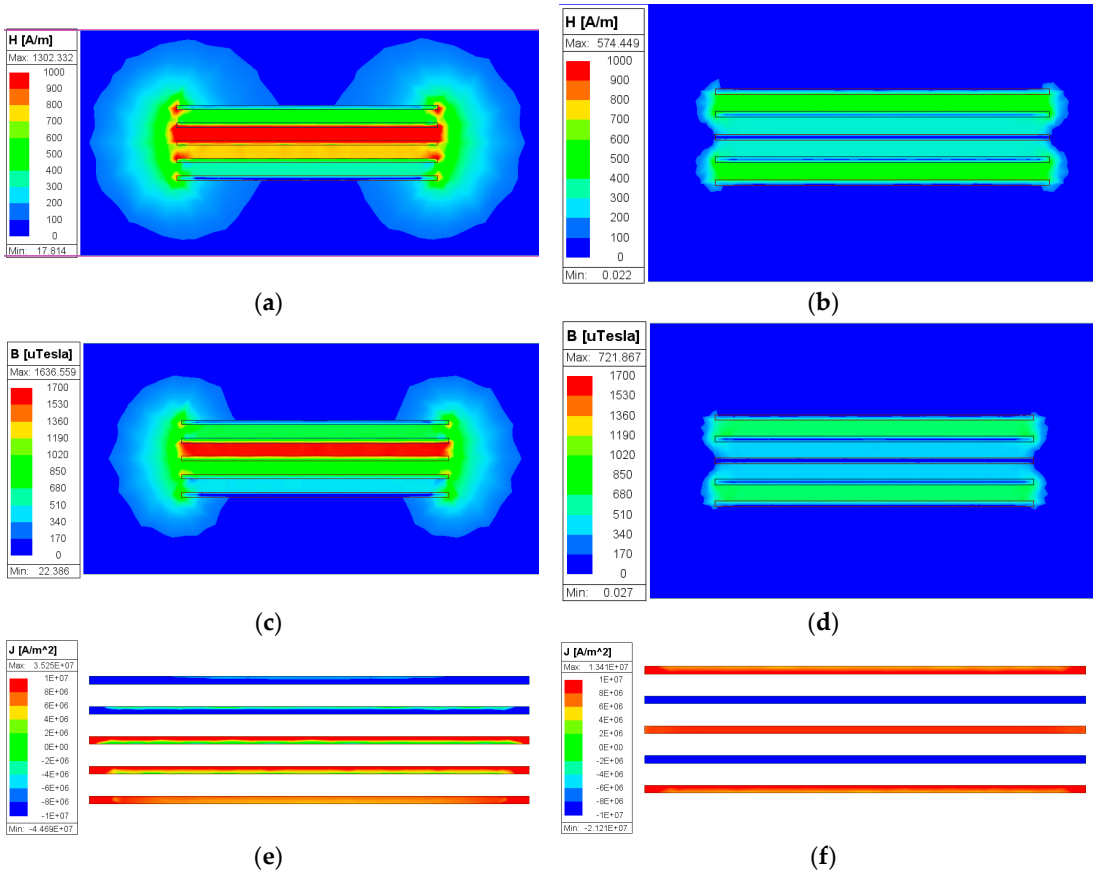

Figure 4. 2D FEA comparison of the segregated (left) and GA-optimized (right) structures at 2 MHz (Np:Ns = 3:2): (**a**,**b**) magnetic field intensity H, (**c**,**d**) magnetic flux density B, and (**e**,**f**) current density J.

4.3. Case 2: High Turns Ratio with Complex Parallel Windings

To further evaluate the algorithm's robustness in handling massive state spaces, an extreme case featuring a high turns ratio and complex parallel structure is introduced: Np:Ns = 9:2, utilizing 2 parallel layers per primary turn and 4 parallel layers per secondary turn, yielding a staggering total of N = 26 physical layers.In such a highly asymmetric structure, finding the optimal sequence is essentially a combinatorial problem of allocating 8 secondary layers into 26 physical slots, expanding the theoretical state space to 1,562,275 possibilities.

To evaluate the algorithm's capability against the combinatorial "curse of dimensionality", an extreme 26-layer asymmetric structure is analyzed in Figure 5.

As depicted in the convergence trajectories [Figure 5b], the proposed GA rapidly navigates the massive discrete search space (over 1.5 million permutations), locking onto the global optimum within 100 generations. The physical mapping of this optimization is starkly illustrated in Figure 2a,c. The conventional segregated baseline suffers from severe monotonic Ampere-turn accumulation, generating a massive spatial MMF peak of 18 at the window center. This extreme field concentration inevitably induces catastrophic localized proximity effect losses.

© 2026 by the author(s). Distributed under a Creative Commons CC BY license.

Preprints.org (www.preprints.org) | NOT PEER-REVIEWED | Posted: 13 May 2026 doi:10.20944/preprints202605.0891.v1

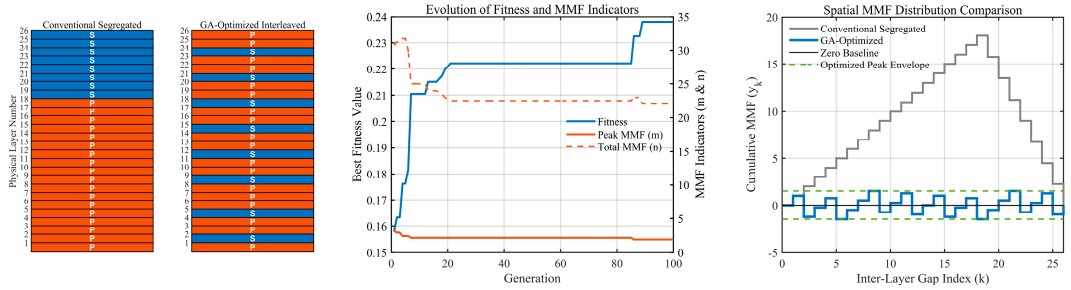

(**a**) (**b**) (**c**)

Figure 5. Optimization of the 26-layer complex structure (Np:Ns = 9:2, e=2, f=4): (a) winding configurations (segregated vs. GA-optimized), (b) GA convergence trajectories, and (c) spatial MMF progression comparison.

In contrast, the GA-optimized sequence breaks manual symmetry rules, deploying a highly non-uniform interleaving strategy [Figure 2a]. This intelligent arrangement ensures prompt local Ampere-turn cancellation, strictly clamping the MMF progression within a minimal ± 1.5 envelope [Figure 2c]. This profound "peak-shaving" effect drastically minimizes the total uncoupled magnetic energy area, physically validating the algorithm's absolute superiority in suppressing high-frequency copper losses and leakage inductance in complex multi-parallel designs.

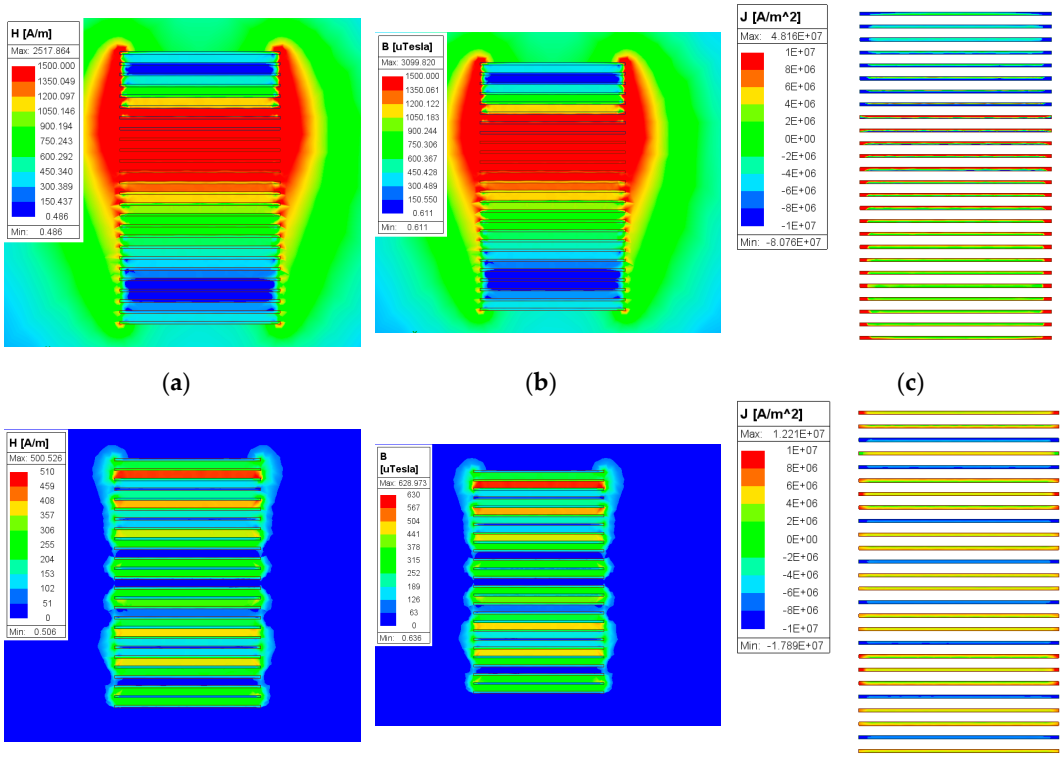

(**a**) (**b**) (**c**)

(d) (**e**) (**f**)

Figure 6. 2D FEA multi-physics comparison of the 26-layer complex structures (Np:Ns = 9:2, e=2, f=4) at 2 MHz: (a–c) magnetic field intensity H, magnetic flux density B, and current density J for the segregated baseline; (d)-(f) corresponding H, B, and J fields for the GA-optimized interleaved configuration.

To physically validate the optimization effectiveness in the extreme 26-layer combinatorial case, 2D FEA was conducted at 2 MHz (primary 2 A, secondary 9 A). Figure 6 compares the multi-physics distributions of the baseline and optimized configurations.

© 2026 by the author(s). Distributed under a Creative Commons CC BY license.

Preprints.org (www.preprints.org) | NOT PEER-REVIEWED | Posted: 13 May 2026 doi:10.20944/preprints202605.0891.v1

In the segregated baseline [Figure 6a–c], severe Ampere-turn accumulation creates a massive magnetic energy concentration at the window center (H_{max} = 2517.8 A/m, B_{max} = 3099.8 uT). This extreme magnetic field induces devastating high-frequency proximity effects, squeezing the current to the conductor surfaces with a peak density of J_{max} = 4.82×10^{7} A/m^{2}, which would inevitably trigger severe thermal runaway in actual multi-layer planar designs. Conversely, the GA-optimized sequence [Figure 6d–f] realizes a highly non-uniform micro-interleaving that thoroughly neutralizes local MMF. The peak magnetic field intensity is drastically suppressed to 500.5 A/m, representing an astonishing 80.1% reduction. Consequently, current crowding is fundamentally eliminated, plunging the peak current density to 1.22 $\times10^{7}$ A/m^{2}. These extreme-case FEA results physically verify the algorithm's absolute dominance in mitigating leakage inductance and high-frequency copper losses for complex multi-parallel transformers.

4.4. Development and Implementation of the Automated EDA Tool

To bridge the massive gap between abstract mathematical heuristic algorithms and practical power electronics engineering, the proposed Constraint-Preserving GA has been packaged into an Automated Electronic Design Automation (EDA) tool. Conventional high-frequency magnetic design heavily relies on manual FEA iterations, which is not only time-consuming but also creates a steep learning curve for engineers dealing with multi-layer parallel structures. The developed tool completely decouples the complex electromagnetic field calculations from the user interface, offering a streamlined, data-driven design workflow.

The graphical user interface (GUI) is systematically developed using MATLAB App Designer, ensuring high compatibility and robust numerical computation capabilities. As illustrated in the operational workflow (Figure 7), the user simply inputs the fundamental transformer specifications, including the turns ratio (Np:Ns) and the number of parallel branches (e, f). The embedded GA engine subsequently initiates the optimization process based on the 1D prefix-sum mathematical model. By automatically applying the Order Crossover (OX) and elitism strategies in the background, the software autonomously navigates the high-dimensional discrete search space without requiring any manual parameter tuning or intervention.

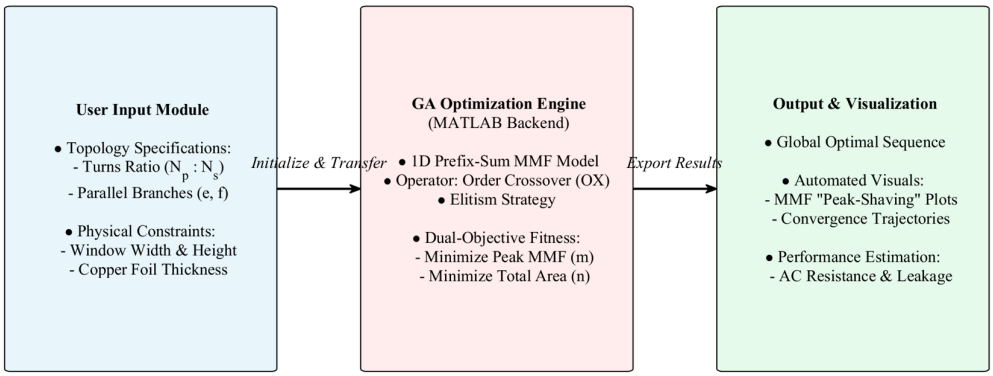

Figure 7. Flowchart of the automated EDA tool for high-frequency planar transformer optimization.

The computational superiority and visualization capabilities of the EDA tool are visually demonstrated in Figure 8. For the extreme 26-layer combinatorial case discussed in Section 4.3, traditional 2D FEA parametric sweeps would require days of continuous computation to traverse even a fraction of the vast design space. In stark contrast, the developed GUI leverages the algorithmic dimensionality reduction to complete the global optimization of over 1.5 million permutations in mere seconds. Furthermore, the interface provides real-time visualization of the spatial MMF prefix-sum progression, immediately plotting the profound "peak-shaving" effect

© 2026 by the author(s). Distributed under a Creative Commons CC BY license.

Preprints.org (www.preprints.org) | NOT PEER-REVIEWED | Posted: 13 May 2026 doi:10.20944/preprints202605.0891.v1

achieved by the globally optimal sequence. This automated software implementation successfully translates the theoretical heuristic algorithm into a highly practical engineering tool, fundamentally accelerating the design and optimization cycle of megahertz-level planar magnetic components.

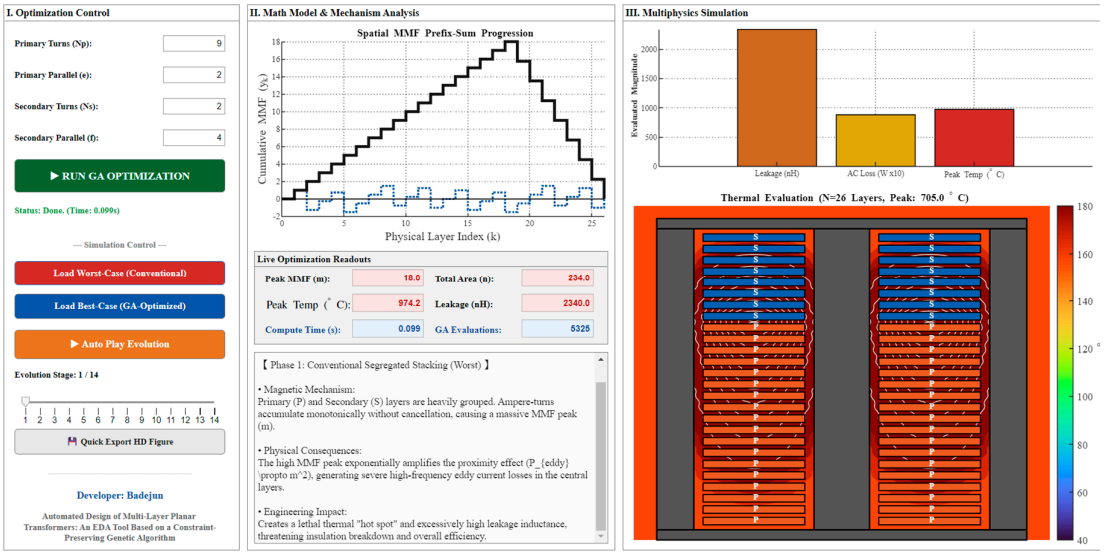

(**a**)

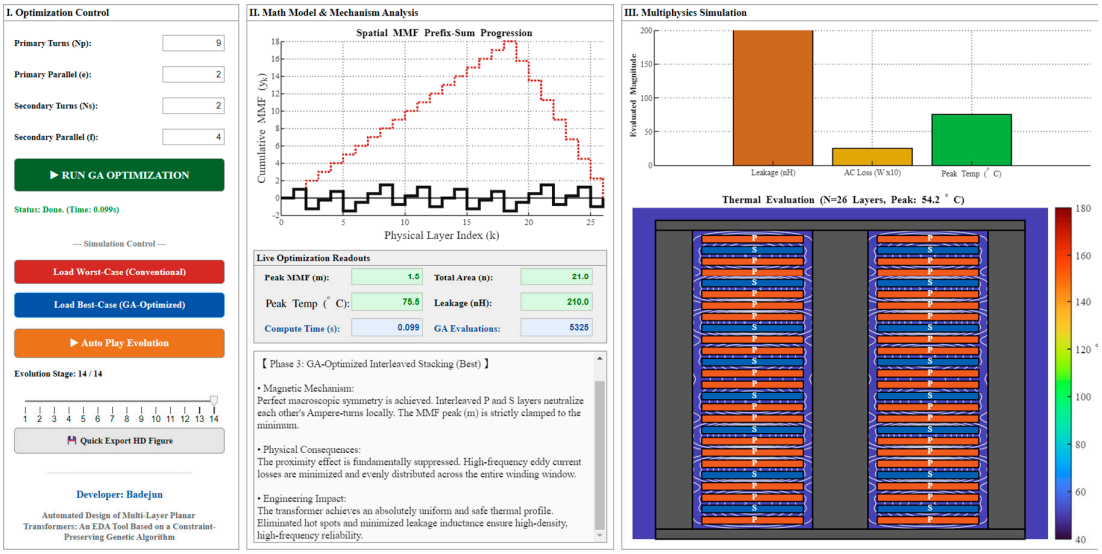

(**b**)

Figure 8. Operational interface and real-time visualization of the developed EDA tool for the extreme 26-layer parallel structure (Np:Ns=9:2, e=2, f=4): (a) the conventional segregated sequence; (b) the GA-optimized interleaved sequence computed in 0.099 seconds, demonstrating a perfectly flattened MMF envelope and a safe, uniform thermal distribution.

To vividly demonstrate the engineering value of the developed software, Figure 8 presents the comprehensive execution interface for the 26-layer extreme combinatorial case. The GUI seamlessly integrates parametric configuration, the 1D mathematical progression model, and surrogate multiphysics visualizations. As captured in Figure 8a, evaluating the conventional segregated arrangement immediately exposes a catastrophic MMF accumulation, which translates into a simulated thermal runaway with a localized peak temperature surging to 705.0 °C. In stark contrast, triggering the GA optimization engine processes over 6,300 evaluations and locks onto the global optimum in a mere 0.099 seconds [see Figure 8b]. The real-time readout explicitly illustrates the "peak-shaving" effect, where the suppressed MMF peak dramatically plummets the projected

© 2026 by the author(s). Distributed under a Creative Commons CC BY license.

Preprints.org (www.preprints.org) | NOT PEER-REVIEWED | Posted: 13 May 2026 doi:10.20944/preprints202605.0891.v1

hotspot temperature to a safe 54.2 °C, alongside substantial reductions in AC loss and leakage inductance. This intuitive, data-driven feedback confirms the tool's absolute superiority in safely and instantly guiding high-frequency magnetic designs without relying on time-consuming finite element iterations.

5. Discussion

The heuristic optimization methodology proposed in this paper successfully bridges the gap between continuous electromagnetic field theory and discrete combinatorial optimization. By mathematically flattening the spatial MMF prefix-sum curve, localized hotspots and proximity effects in high-frequency planar transformers are fundamentally eliminated. However, in engineering practice, fabricating extreme configurations—such as the 26-layer interleaved PCB transformer presented in Case 2—introduces additional manufacturing and layout challenges, including complex via placements, high-voltage insulation clearances, and increased inter-layer parasitic capacitance. While the baseline hardware experiments have successfully validated the core mechanism of the proposed algorithm in reducing leakage inductance and improving efficiency, the extreme 26-layer globally optimal physical prototype has not yet been fabricated and tested in this current study. Future research will focus on integrating 3D PCB routing and parasitic capacitance constraints into the GA fitness evaluation, alongside the comprehensive system-level hardware validation of this extreme high-turns-ratio prototype.

6. Conclusions

To address the computational "curse of dimensionality" encountered in the design of multi-layer parallel windings for high-frequency planar transformers, this paper proposes a universal, data-driven Electronic Design Automation (EDA) methodology. The main conclusions are as follows:

1. A one-dimensional prefix-sum mathematical model is established, rigorously reducing the complex 3D electromagnetic field evaluation into a discrete algebraic sequence calculation. This provides a computationally lightweight foundation for quantitatively assessing leakage inductance and proximity effect losses.

2. A customized Genetic Algorithm (GA) featuring Order Crossover (OX) and an elitism strategy is introduced. It achieves highly efficient global optimization within massive discrete spaces while guaranteeing 100% physical validity of the winding structures.

3. Validated by an extreme 26-layer complex parallel case, the proposed algorithm successfully bypasses over 1.5 million permutations within 100 generations. The derived global optimum slashes the MMF peak by nearly 80%, thoroughly eliminating localized thermal hotspots.

This research fundamentally replaces the human-intuition-dependent empirical trial-and-error methods in conventional high-frequency magnetic design, offering a scalable, intelligent design pathway for the development of megahertz-level, high-power-density converters.

Author Contributions: Conceptualization, D.B. and X.L.; methodology, D.B.; software, D.B.; formal analysis, Y.W.; investigation, F.Y.; writing—original draft preparation, D.B.;.

Funding: This research received no external funding.

Data Availability Statement: The data presented in this study and the algorithmic EDA tool are available on request from the corresponding author.

Conflicts of Interest: The authors declare no conflicts of interest.

© 2026 by the author(s). Distributed under a Creative Commons CC BY license.

Preprints.org (www.preprints.org) | NOT PEER-REVIEWED | Posted: 13 May 2026 doi:10.20944/preprints202605.0891.v1

Abbreviations

The following abbreviations are used in this manuscript:

1D	One-dimensional
EDA	Electronic Design Automation
FEA	Finite Element Analysis
GA	Genetic Algorithm
HFPTs	High-frequency planar transformers
MMF	Magnetomotive force
OX	Order Crossover
PCB	Printed circuit board

References

1. C. Fei, F. C. Lee, and Q. Li, "High-Efficiency High-Power-Density LLC Resonant Converter With an Integrated Planar Transformer for High-Output Current Applications," IEEE Transactions on Power Electronics, vol. 32, no. 12, pp. 9071-9082, 2017.
2. Z. Ouyang and M. A. E. Andersen, "Overview of Planar Magnetic Technology—Fundamental Properties," IEEE Transactions on Power Electronics, vol. 29, no. 9, pp. 4888-4900, 2014.
3. J. Wei, et al., "A Novel Low-Winding-Loss Circulated Interleaving Structure for Planar Transformers Based on Current Invariance Principle," IEEE Transactions on Transportation Electrification, vol. 11, no. 1, pp. 592-609, 2025.
4. Z. Ouyang, G. Sen, O. C. Thomsen, and M. A. E. Andersen, "Design and optimization of planar transformer in high-power DC-DC converters," IEEE Transactions on Industrial Electronics, vol. 59, no. 7, pp. 2800-2810, 2012.
5. C. Hou, F. Xue, P. Li, X. Yang, and T. Q. Zheng, "Design and Analysis of a High-Frequency and High-Efficiency Planar Transformer," IEEE Transactions on Magnetics, vol. 56, no. 2, pp. 1-6, Feb. 2020.
6. M. Mu, F. C. Lee, Q. Li, and D. Gilham, "A High-Frequency, High-Current, Low-Profile, GaN-Based LLC Resonant Converter," IEEE Journal of Emerging and Selected Topics in Power Electronics, vol. 4, no. 3, pp. 854-862, Sept. 2016.
7. D. Han, S. Li, Y. Wu, M. Haley, and B. Sarlioglu, "Performance Evaluation of Up to 1 MHz SiC-Based Isolated Resonant DC–DC Converter," IEEE Transactions on Industry Applications, vol. 53, no. 6, pp. 5652-5663, Nov.-Dec. 2017.
8. E. A. Jones, F. Wang, and D. Costinett, "Review of Commercial GaN Power Devices and GaN-Based Converter Design Challenges," IEEE Journal of Emerging and Selected Topics in Power Electronics, vol. 4, no. 3, pp. 707-719, Sept. 2016.
9. T. Wang and J. Yuan, "Improvement on Loss Separation Method for Core Loss Calculation Under High-Frequency Sinusoidal and Nonsinusoidal Excitation," IEEE Transactions on Magnetics, vol. 58, no. 8, pp. 1-9, 2022.
10. C. Li, M. Cheng, and W. Wang, "A New Two-Dimensional Electromagnetic Field Analysis and Loss Calculation Method for High-Frequency Applications Based on Vector Magnetic Circuit Theory," Energies, vol. 18, p. 2639, 2025.
11. W. G. Hurley, E. Gath, and J. G. Breslin, "Optimizing the AC resistance of multilayer planar transformers," IEEE Transactions on Power Electronics, vol. 15, no. 2, pp. 369-373, 2000.
12. Z. Ouyang, O. C. Thomsen, and M. A. E. Andersen, "Optimal Design and Tradeoff Analysis of Planar Transformer in High-Power DC–DC Converters," IEEE Transactions on Industrial Electronics, vol. 59, no. 7, pp. 2800-2810, 2012.
13. M. A. Saket, M. Shafiei, and M. Ordonez, "Planar Transformers with Unequal-Turn Layers for Thermal-Constrained High-Frequency LLC Converters," IEEE Transactions on Power Electronics, vol. 36, no. 1, pp. 835-849, 2021.
14. Y. Chen, et al., "Integrated Fractional-Turn Planar Transformer for MHz and High-Current Applications," IEEE Transactions on Power Electronics, vol. 38, no. 6, pp. 7533-7544, 2023.

© 2026 by the author(s). Distributed under a Creative Commons CC BY license.

Preprints.org (www.preprints.org) | NOT PEER-REVIEWED | Posted: 13 May 2026 doi:10.20944/preprints202605.0891.v1

15. X. Zhou, et al., "A Design Method of Partially Interleaved Winding Structure With Low Leakage Inductance for Planar Transformer Application," IEEE Transactions on Power Electronics, vol. 38, no. 5, pp. 6366-6379, 2023.
16. Z. Zhao, M. Ouyang, M. C. Duffy, et al., "An Improved Partially Interleaved Transformer Structure for High-Voltage High-Frequency Multiple-Output Applications," IEEE Transactions on Industrial Electronics, vol. 66, no. 4, pp. 2691-2702, 2019.
17. D. Ba, F. Yu, Y. Wang, et al., "Optimization Study of Parasitic Parameters in Parallel Interleaved Windings for High-Frequency PCB Transformers," IEEE Transactions on Power Electronics, vol. 40, no. 10, pp. 14894-14907, 2025.
18. M. Guacci, D. Bortis, and J. W. Kolar, "Optimized Design of Multi-MHz Frequency Isolated Auxiliary Power Supply for Gate Drivers in Medium-Voltage Converters," IEEE Transactions on Power Electronics, vol. 35, no. 8, pp. 8303-8321, 2020.
19. E. Agirman and F. G. Uzun, "A New Optimization Method for Gapped and Distributed Core Magnetics in LLC Converter," IEEE Transactions on Power Electronics, vol. 38, no. 5, pp. 6165-6178, 2023.
20. C. H. Chen, et al., "Automated Design and Optimization of Planar Transformers for High-Frequency Applications," in 2023 IEEE 14th International Symposium on Diagnostics for Electrical Machines, Power Electronics and Drives (SDEMPED), pp. 1-7, 2023.

Disclaimer/Publisher's Note: The statements, opinions and data contained in all publications are solely those of the individual author(s) and contributor(s) and not of MDPI and/or the editor(s). MDPI and/or the editor(s) disclaim responsibility for any injury to people or property resulting from any ideas, methods, instructions or products referred to in the content.

© 2026 by the author(s). Distributed under a Creative Commons CC BY license.